Journal of Himalayan Earth Sciences Volume, No., 2026 pp. 1-19

Petrographic and Geotechnical Characterization of Calcitic Marble from the Kashala Formation, Lower Swat, Khyber Pakhtunkhwa, Pakistan

Sami Ullah[1], Rafique Ahmad[1*], Asher Samuel Bhatti[1], Fahad Ali[1], Manzoor Ahmad[2] and Badshah Hussain[1]

[1]*Department of Geology, Bacha Khan University Charsadda, Khyber Pakhtunkhwa, 24420, Pakistan*

[2]*Department of Agriculture, Bacha Khan University Charsadda, Khyber Pakhtunkhwa, 24420, Pakistan*

*****Corresponding author: *rafique.ahmad@bkuc.edu.pk*

Submitted Date:11/11/2025 Acceptance Date: 24/06/2026 Publication Date:---------

Abstract

This study evaluates the petrographic and geotechnical properties of calcitic marble of the Kashala Formation exposed in the Palai (Dargai) and Barikot (Swat), Khyber Pakhtunkhwa, Pakistan. The bulk rock samples and aggregate were collected from three different quarries in the Palai area and two quarries in the Swat Barikot area. Mineralogically, the Kashala Formation comprises recrystallized calcite, plagioclase, muscovite, and biotite as essential minerals; quartz, epidote, and sericite as accessory minerals, while chlorite and opaque minerals in trace amounts. Quartz grains exhibit overgrowth and intra-granular fractures, showing deformation-related recrystallization. The petrographic investigation shows textural uniformity. The investigated geotechnical tests include unconfined compressive strength (UCS), unconfined tensile strength (UTS), shear strength, point load, soundness, alkali-silica reaction (ASR), alkali-carbonate reaction (ACR), Los Angeles abrasion (LA), water absorption, porosity, specific gravity, and impact value. The obtained average results of UCS are 36.9, 39.5, 42.5, 40.9, and 33.06 MPa for bulk samples A, B, C, D, and E, respectively. Similarly, the obtained average results of UTS are 7.94, 8.8, 10.55, 6.85, and 4.97 MPa for bulk samples A, B, C, D, and E, respectively. The average values for soundness and point load are 2.45% and 3.31 MPa, respectively. The average values for LA, water absorption, porosity, specific gravity, and impact value are 27%, 0.60%, 1.79%, 2.68%, and 17.65%, respectively. Overall, the studied rocks fall within the moderate to moderately strong categories, and aggregates show acceptable properties to be utilized in engineering projects.

Keywords: Kashala Formation; Rock aggregate; Petrography; Geotechnical properties.

1. Introduction

Historically, marble has remained the primary rock used in construction and decorative applications. Its widespread use since antiquity is attributed to its durability, ability to achieve a polished finish, diverse aesthetic colors, and ease of processing (Xeidakis and Samaras, 1996). The extraction and commercial distribution of marble have increased significantly over recent decades due to advancements in technology and quarrying methods.

Aggregates must meet specific requirements, and only a limited number of geological formations meet these criteria. Aggregates possess diverse physical and chemical properties that determine their suitability for construction applications. The quality of aggregate is closely linked to the properties of the source rock (Koukis et al., 2007). The geological characteristics of aggregate, regardless of application, significantly affect its performance (Hartley 1974; Lees and Kennedy, 1975; Smith and Collis, 2001). The physico-mechanical properties of aggregate result from its geological history, including the rock origin and subsequent processes like folding, faulting, jointing, hydrothermal alteration and weathering. Geological parameters, as defined by lithological classification, are essential for evaluating the physical and chemical characteristics that influence the engineering behavior of aggregate. Although various rock types may serve as aggregate resources depending on their physical properties and transportation costs, marble and limestone are among the most significant construction materials.

The initial significant marble reserves in Pakistan were discovered in the Mullagori and Swabi regions of Khyber-Pakhtunkhwa province (KP), Pakistan. Commercial exploitation and the subsequent establishment of the marble industry in Pakistan began in the late 1960s (SMEDA, 2007). Marble deposits in Pakistan are generally classified into three categories: a) crystalline calcite and/or dolomite, b) partially crystallized dense compact limestone, and c) travertine deposits. Additionally, serpentine marble has been identified in Pakistan and Azad Kashmir (Ahmad, 1969). KP contains approximately 98% of the total 3.0 billion-ton reserves and produces nearly 87% of the marble in the country. The principal marble occurrence belts identified in KP are the Mardan-Buner belt, the Swabi-Nowshera belt, the Swat-Kohistan belt, and the southern district belt (Khan et al., 2017).

Besides these, huge reserves have also been reported from the Reshun, Shoghore, Gahiret, and Shishi valleys of Chitral (Kazmi and Abbas, 2001; Afridi, 2004). All of these marbles were extracted from deposits of Devonian to Jurassic carbonate rocks, which form part of the Indian plate sequence and constitute the footwall of the Main Mantle Thrust (MMT). Pakistan produces more than 70 types of marble, but their exact quality, chemical, petrographic, and engineering properties are not fully known.

This paper presents the petrographic and geotechnical properties of the calcitic marbles of the Kashala Formation (Fig. 1). This study analyzes the petrography and textures of rock samples from the Palai and Barikot areas to elucidate rock strength based on mineralogical composition and geotechnical characterization. This research further examines the physical and mechanical properties of these rocks to assess the strength of the selected samples. Mohr diagrams are subsequently constructed to facilitate the interpretation and evaluation of the shear strength characteristics of the samples.

2. Tectonic Setting and Stratigraphy

The Indian plate, the Eurasian plate, and the Kohistan Island Arc (KIA) are the three separate tectonic zones that define northern Pakistan. The Main Karakoram Thrust (MKT), also known as the Shyoke suture zone, formed as a result of the KIA's initial collision with the Eurasian plate during the Cretaceous period (Searle et al., 1999; Schaltegger et al., 2002). Later on, the Indian plate collided with the KIA and formed the MMT, or Indus suture zone. The MMT was expanded from Afghanistan to Babusar in the east and then to Ladakh in the north, circling the Nanga Parbat Massif (DiPietro et al., 2000). The KIA consists of Cretaceous and Eocene plutonic belts, granulites, calc-alkaline gabbronorite pyroxene, volcanic, amphibolites, and minor metasediments (Coward et al., 1986; Johnson and DeGraff, 1988).

The KIA comprises six geological units: the Jijal Complex, Kamila Amphibolites, Chilas Complex, Kohistan Batholiths and Gilgit Gneisses, Chalt Volcanic, and Yasin Group Metasediments, which are aligned from south to north. The mafic and ultramafic rocks of the Jijal Complex exhibit a transition from upper mantle to lower crustal compositions (Jan and Howie, 1981; Ringuette et al., 1999; Dhuime et al., 2007). The Kamila Amphibolites have been divided by the Chilas complex into two parts: the southern Kamila Amphibolite, and the northern Kamila Amphibolite belt facies (Khan et al., 1997). The Kamila amphibolite mainly contains metaplutonic, metavolcanic rocks, and amphibolite facies rocks.

Kazmi et al. (1984) assigned the name Alpurai schist for calcareous-rich schistose rocks that are situated atop the Manglaur Formation and the Swat Granitic Gneiss in an unconformable manner. DiPietro (1990) introduced the group status to Alpurai schist and subdivided the Alpurai group into the Marghazar, Kashala, Saidu, and Nikani Ghar Formations (Fig. 2). The Marghazar Formation in the Swat area is continuously covered by the Kashala, Saidu, and Nikani Ghar Formations. The Marghazar Formation closely resembles the Kashala Formation; however, it is unique within the Alpurai group for containing amphibolites. In addition, the Kashala, Saidu, and Nikani Ghar Formations have substantial lithological similarities.

The Kashala Formation covers a large area along the Dosara Syncline. The type locality of the Kashala Formation is about 13 km SSW of Saidu in Swat. There occur significant changes in the grade of metamorphism in the Kashala Formation from north to south.

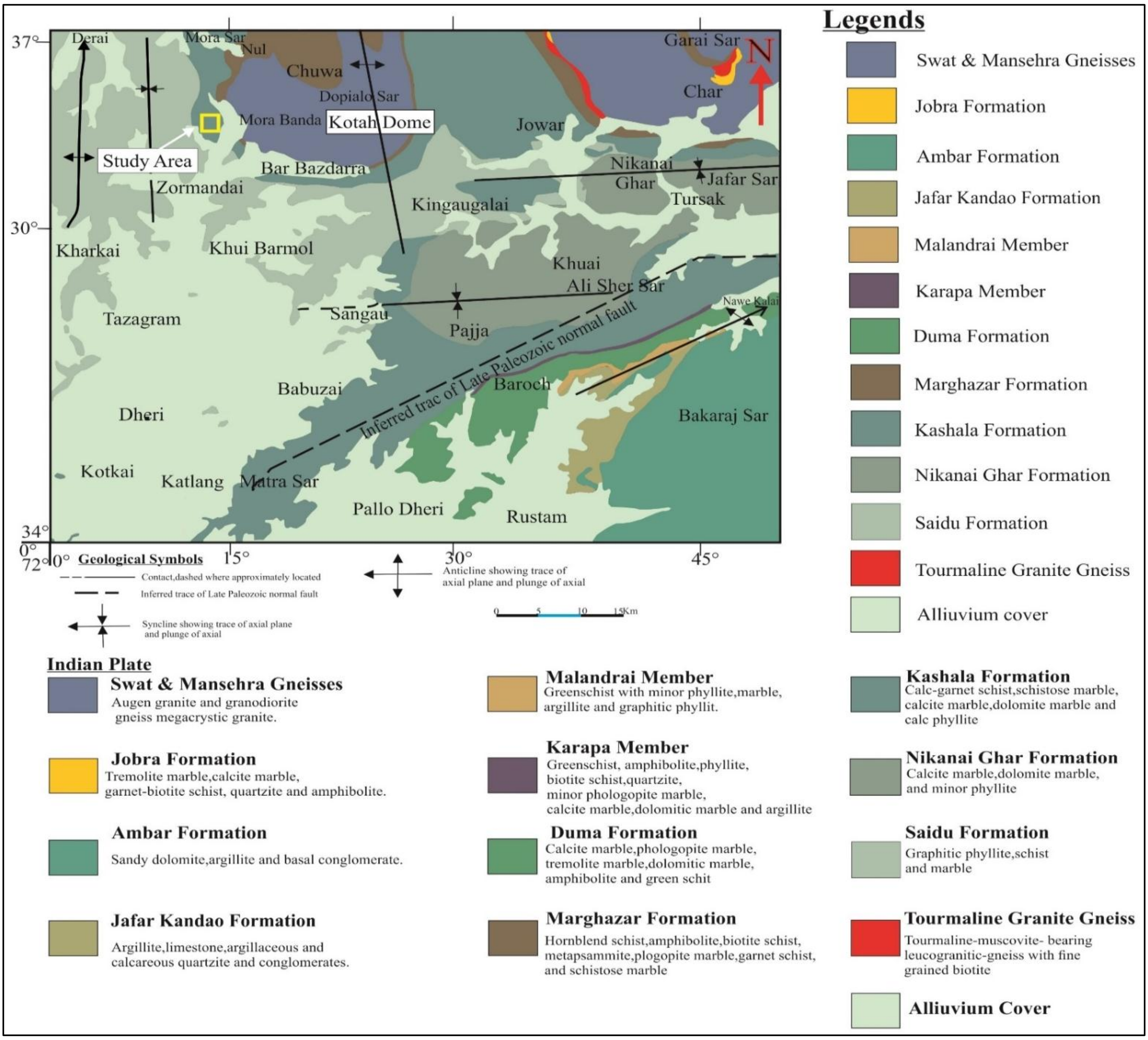

Fig. 1. Regional geological map showing the structures and stratigraphy exposed in north western Himalayas, Pakistan. Rectangle shows the study area (redrawn after Hussain et. al., 2004).

At the type locality, the Kashala Formation comprises garnet- and epidote-rich calc-schist, schistose marble, and brown-weathering calcitic marble that is mostly coarsely crystalline. North of Baroch, the Kashala Formation comprises dolomitic marble and brown-weathering marble, with minor intercalated phyllites. North of Jowar, the formation is less than 700 m thick, whereas near Baroch, the observed thickness exceeds 1200 m. The amphibolite horizon of the Marghazar Formation and the lower Kashala Formation contact are sharp. Towards the east, in the vicinity of Sipar and Bagra, intercalated graphitic phyllite is common within the Kashala Formation. Further east, much of the undifferentiated Alpurai group is considered part of the Kashala Formation.

3. Methodology

Five representative bulk samples and different-sized aggregates of the Kashala Formation were collected from two different study areas (Palai and Barikot) of the Lower Swat region.

Among the five bulk samples, three (Bulk samples A, B, and C) were collected from the Palai area, whereas two (Bulk samples D and E) were obtained from the Barikot area. The samples were cored with the help of a core drilling machine in the Geotechnical Laboratory of the National Centre of Excellence in Geology, University of Peshawar. Five core samples were drilled from bulk sample (A), three cores drilled from bulk sample (B), two cores from bulk sample (C), two cores from bulk sample (D), and three cores from bulk sample (E). Each core sample was selected for thin section preparation. A total of fifteen thin sections were prepared to describe petrographic characteristics, and the grain counting technique was employed for mineral quantification.

To evaluate mechanical characteristics such as UCS, UTS, and point load, cylindrical samples were made in compliance with ASTM standards (D 7012-14, D 3967-16, D 5731).

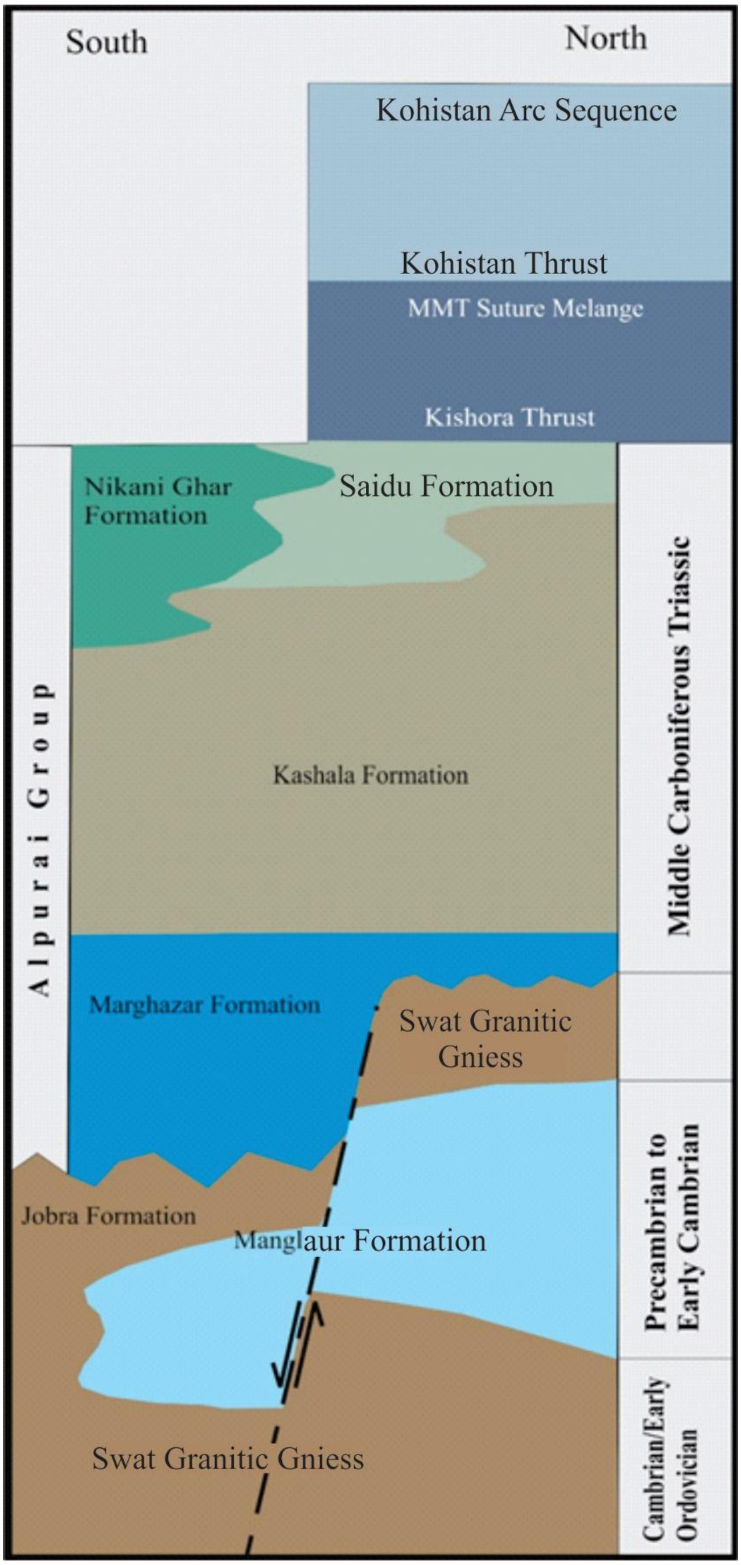

Fig. 2. Stratigraphic column of the study area showing different formations of Alpurai Group Metasediments (AGM; After DiPietro et al. (1993).

Furthermore, from UCS and UTS values, shear strength, cohesion, and the internal angle of friction were determined. The aggregate was used for chemical analysis like soundness, ASR and ACR according to the ASTM specifications (C 88, C 1260, C 586), and physical analysis such as Los Angeles Abrasion (LLA), porosity, specific gravity, water absorption and impact value were in accordance with standards (ASTM C 131, ASTM C 830, ASTM C 127-88, BS 882). For regression analysis, the data were organized in an Excel spreadsheet, and graphs were generated using Microsoft Word.

4. Results

4.1. Petrography

Microscopic study of selected specimens contains recrystallized calcite and plagioclase as essential minerals and muscovite, biotite, and quartz as accessory minerals, while epidote and opaque minerals are present in trace amounts. Calcite is the most dominant phase, and its proportion ranges from ~52-63% in the studied specimens (Table 1). The calcite grains are angular to subangular and elongated to anhedral and rhombohedral in shape (Figs. 3a, b). The lamellar twining is present in calcite, which occurs due to deformation and shows a recrystallized nature, representing prograde metamorphism in the region (Figs. 3a, b). A few of the calcite grains are slightly fractured and unaltered. The inclusions of opaque minerals were also noted inside the calcite crystal (Figs. 3a, 4b).

Plagioclase is the second dominant constituent, ranging from ~15 to ~26% (Table 1). Plagioclase grains are mostly elongated and euhedral to subhedral in shape (Figs. 3b, 4a, d). One of the most important features in plagioclase is polysynthetic twinning, which is developed due to the deformation event. Low relief, colorless nature, and polysynthetic twinning are the diagnostic features of plagioclase (Figs. 3b, 4d). Within the plagioclase crystals, inclusions of opaque minerals were noted in rounded shapes (Fig. 3b). In most of the places, the plagioclase grains are altered to epidote and clay minerals following the phenomena of epidotization and saussuritization, respectively (Fig. 3d). Some of the plagioclase crystals are also converted into microcline due to alteration (Fig. 4c).

Table 1: Modal Mineralogical composition of selected samples. The mineral abbreviations are used following the guidelines given by Whitney and Evans (2010).

Locality		Sample No.	Cal	Pl	Ms	Bt	Qz	Ep	Opq
Palai Area	Bulk Sample "A"	A1	55	20	10	7	7	-	1
		A2	50	14	6	10	15	-	5
		A3	68	20	2	3	6	-	>1
		A4	40	35	11	12	>1	-	>1
		A5	50	35	3	5	2	-	5
		Average	52.6	24.8	6.4	7.4	6.2	-	2.6
	Bulk Sample "B"	B1	80	10	2	6	-	-	2
		B2	40	30	10	7	7	-	6
		B3	70	13	5	7	>3	-	2
		Average	63.33	17.66	5.66	6.66	3.33	-	3.33
	Bulk Sample "C"	C1	65	15	4	8	6	1	>1
		C2	60	20	4	3	8	-	5
		Average	62.5	17.5	4	5.5	7	1	3
Barikot Area	Bulk sample "D"	D-1	55	20	5	7	10	1	2
		D-2	50	25	10	5	5	1	4
		Average	52.5	22.5	7.5	6	7.5	1	3
	Bulk sample "E"	E-1	56	23	4	3	7	0	7
		E-2	59	28	2	1	8	1	1
		E-3	52	27	3	2	10	0	6
		Average	55.66	26	3	2	8.33	0.33	4.66

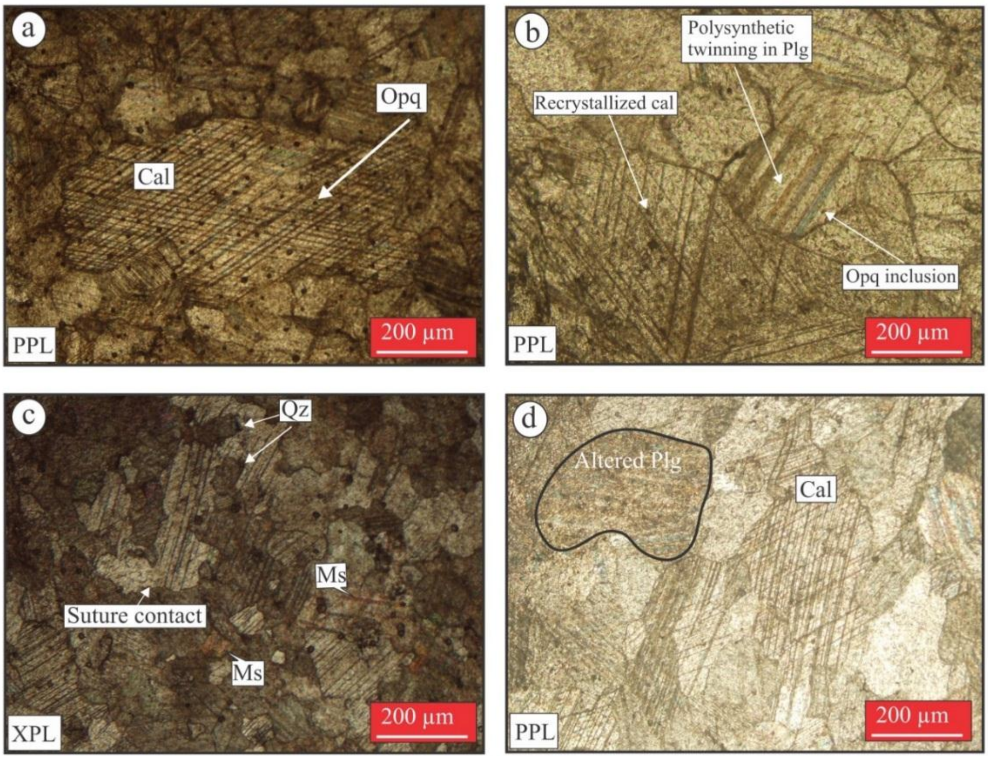

Fig. 3. Photomicrographs: (a) Well-developed recrystallized twinned calcite; (b) Polysynthetic twinning in plagioclase with opaque inclusions; (c) Quartz grains are irregularly arranged in calcite crystal. Suture contact between grains and muscovite flakes is observed (d) Altered plagioclase.

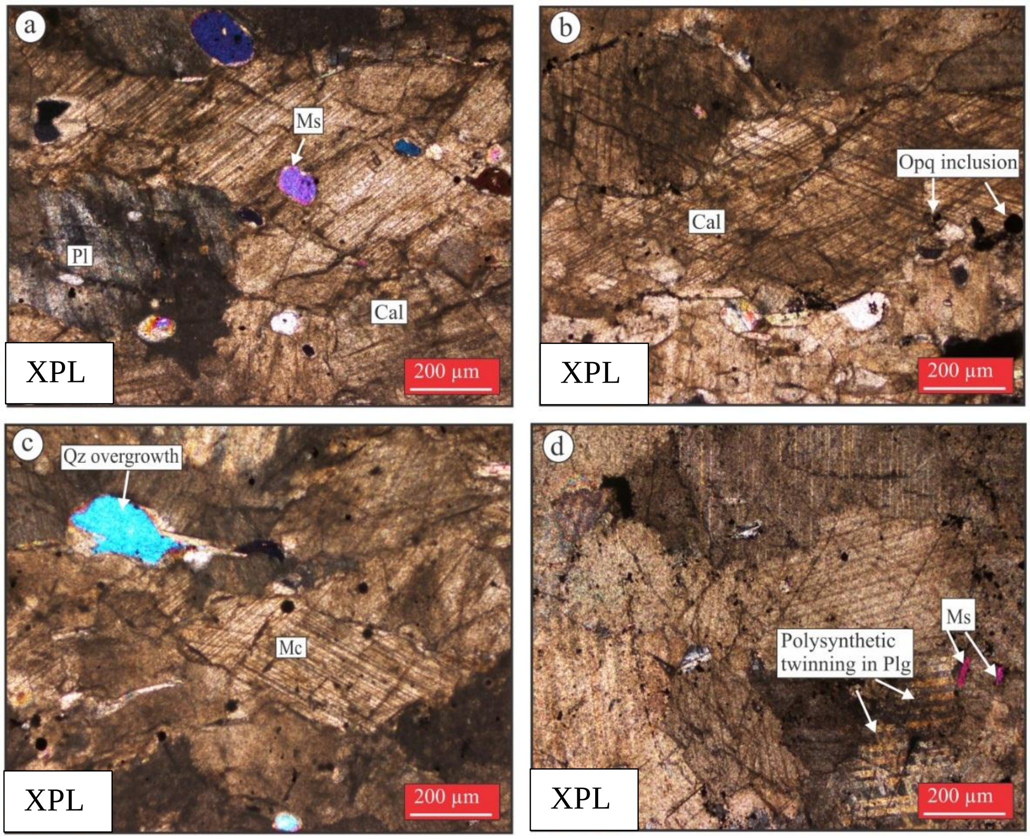

Fig. 4. Photomicrographs: (a) Polysynthetic twinning in plagioclase, biotite, and quartz; (b) well-developed recrystallized twinned calcite with opaque inclusions; (c) Overgrown quartz grains are irregularly arranged in calcite crystal and microcline crystal; (d) Polysynthetic twinning in plagioclase and muscovite flakes is observed.

The muscovite flakes observed in different thin sections range from 3-6% (Table 1). The shape of muscovite varies in the studied thin sections but is mostly found to be flaky in shape. Straight cleavages were also noted in muscovite grains (Figs. 3c, 4d). Multiple grains of biotite were studied, ranging from 2-6% (Table 1). The shape of biotite is euhedral to anhedral, but most commonly it is present in a tabular or irregular shape (Fig. 4a).

Quartz grains exhibit rounded to sub-rounded shapes and exhibit undulose extinction (Fig. 4c). Most of the quartz grains have suture contact with other grains. The outlines or boundaries are irregular or concave (Fig. 3c). Furthermore, quartz grains with intra-granular inclusions are also observed (Fig. 4a). Opaque minerals are found in trace amounts ranging from 1-5% (Table 1).

4.2. Geotechnical Characteristics

4.2.1. Unconfined or Uniaxial Compressive Strength (ASTM D 7012-14)

When unidirectional stress is applied to a rock sample, usually along the axial direction of its ends, the maximum pressure that the sample can tolerate is known as UCS (Bell, 2007). The compression of the cylindrical rock samples occurs parallel to their longitudinal axis in the UCS test (Jaeger and Cook, 1976). Determining the UCS of a core sample with regular geometry requires entire rocks for excellent quality, because extensively fractured, foliated, weak, and thinly bedded rocks cannot yield cores of standard grade (Zorlu et al., 2008). The obtained results from the studied samples are given in Table 2.

4.2.2. Unconfined Tensile Strength (ASTM D 3967-16)

Tensile strength is calculated by dividing the maximum stress a disc-shaped sample can withstand during stretching by its actual cross-sectional area. The highest stress a material specimen can sustain during a tensile test before rupturing under particular circumstances is known as UTS. This is the highest tensile stress that a rock specimen can withstand. A rock's resistance to compression is significantly greater than its resistance to tension (Bell, 2007). The ability of a rock to withstand fracture under tension is measured by its tensile strength (Din et al., 1993). Analyzed samples are shown in Table 2.

4.2.3. Shear Strength

Shear strength can be defined as the maximum resistance a rock offers to deformation resulting from continuous shear displacement under an applied shear force (Jumikis, 1983). Rocks resist shear stress by two internal mechanisms:

(i) The internal angle of friction (Φ) (Figs. 5-7) is the internal friction or resistance to movement along the sliding surface, as well as the interlocking of individual rock grains.
(ii) The internal bonding of rock is mainly measured by the cohesion factor, which is denoted by C (Figs. 5-7). Cohesion is the natural shear strength of materials when no outside forces are acting on them (Zorlu et al., 2008).

4.2.4. Point Load Test (ASTM D 5731)

UCS is one of the most important strength measurements for characterizing rock materials. Indirect testing methods are commonly employed to estimate UCS, as conventional laboratory experiments require precisely machined specimens. Several researchers (Brook, 1985; Ghosh and Srivastava, 1991; Chau and Wong, 1996; Tuğrul and Zarif, 1999; Basu and Aydin, 2006) have referred to the point load test as the most competent tool in this regard. The geomechanics classification of rock masses (Rock Mass Rating System) has even included the point load strength as a substitute for the UCS of intact material to rate the rock strength (Bieniawski, 1989). But aside from UCS prediction, its potential has not been fully realized in a typical rock engineering setting.

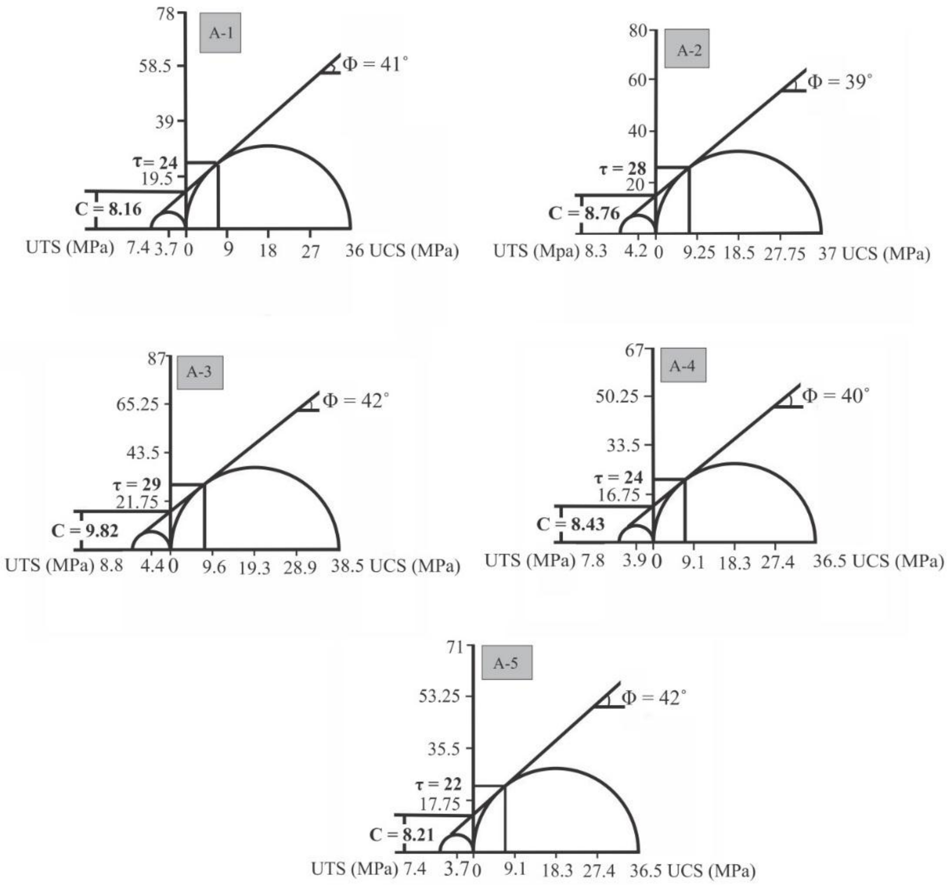

Fig. 5. Mohr diagrams of specimens A-1 to A-5 showing shear strength of bulk sample A.

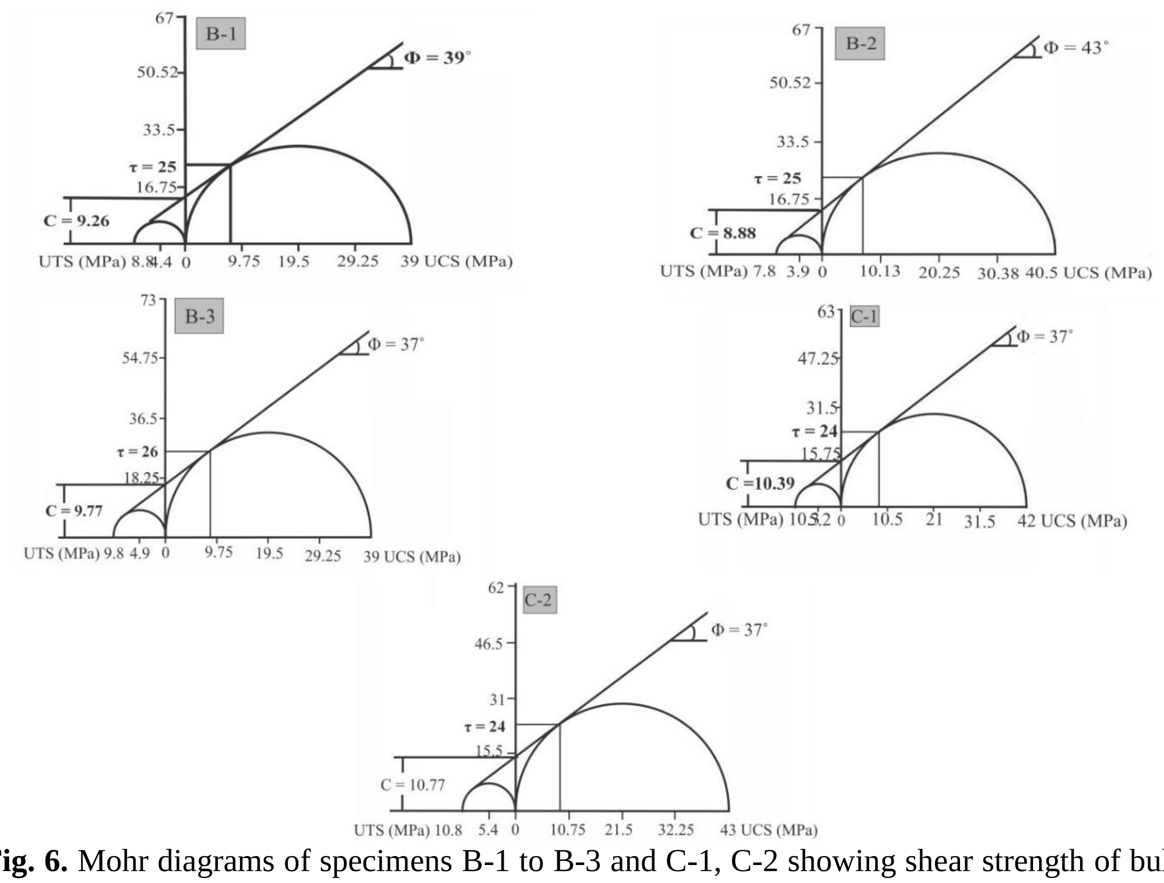

Fig. 6. Mohr diagrams of specimens B-1 to B-3 and C-1, C-2 showing shear strength of bulk samples B and C, respectively.

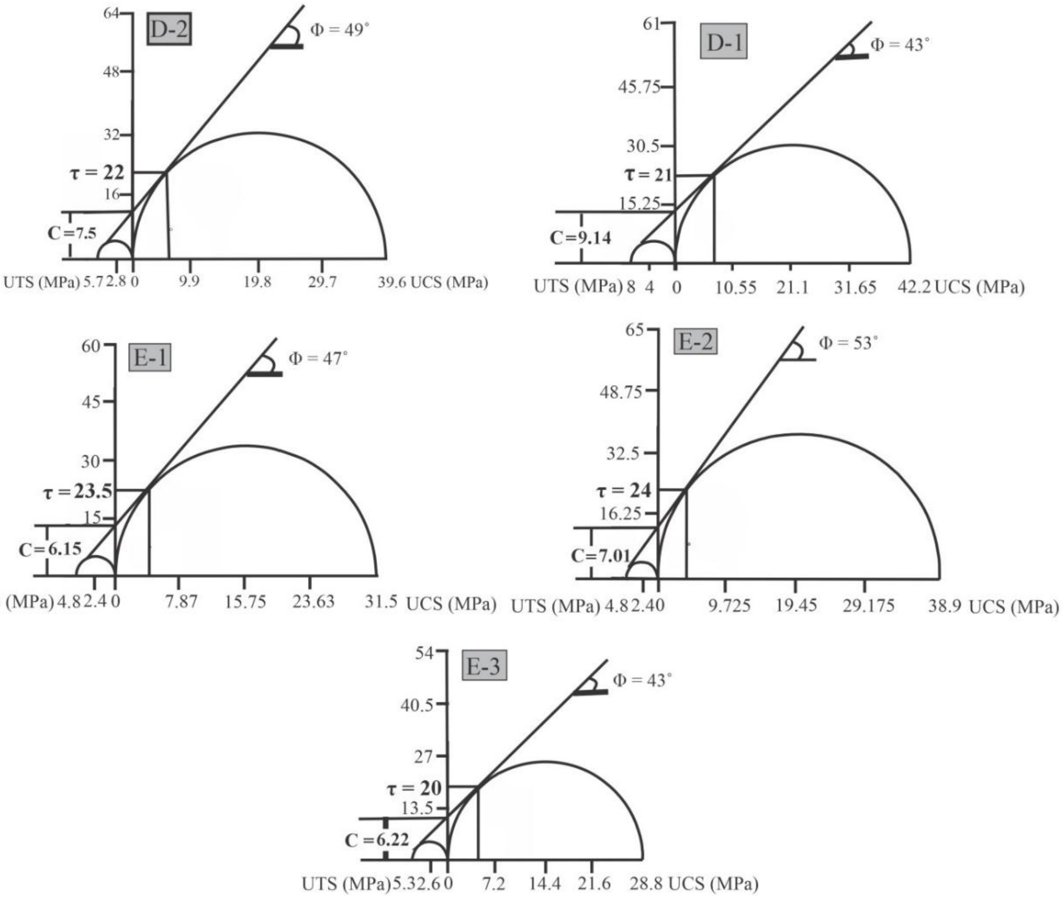

Fig. 7. Mohr diagrams of specimens D-1, D-2 and E-1, E-3 showing shear strength of bulk samples D and E, respectively.

In the current research, point load index is determined for Bulk Samples D and E from Barikot, Swat, whereas Bulk Samples A, B, and C are not analyzed for point load index. The analyzed sample results are given in Table 2

4.2.5. Soundness test (ASTM C 88)

The soundness test evaluates the effects of climatic conditions such as freezing, thawing, drying, and wetting on aggregate, and assesses its resistance to breakdown and disintegration. When concrete and asphalt are covered, weathering cycles have no effect till the covering is unbroken. During compaction, soft and weak rocks are readily broken down. Therefore, it is necessary to select durable aggregates (Wu et al., 1998). The soundness test is determined by using the saturated sodium Sulphate solution (Na_2SO_4) in which the aggregate is immersed repeatedly. After that, the salt that precipitated in the pore spaces is either fully or partially dehydrated by oven drying. It measures the resistance of aggregates to disintegration. In the current research, the analyzed sample values are given in Table 3.

4.2.6. Alkali-Silica Reaction in Aggregate Concrete (ASTM C 1260)

The ASR, also known as concrete cancer, is a detrimental swelling reaction that occurs in concrete over time. This reaction happens between the highly alkaline cement paste and non-crystalline silica found in common aggregates when exposed to sufficient moisture. ASR in aggregate refers to a chemical reaction between reactive silica in certain aggregates and alkali hydroxides in the pore fluid of concrete. This reaction can cause expansion and cracking of the concrete over time, leading to structural problems and sometimes necessitating destruction. ASR is the most common form of alkali-aggregate reaction in concrete, and it is caused by the reaction between hydroxyl ions in the alkaline cement pore solution in the concrete and reactive forms of silica in the aggregate, such as chert, quartzite, opal, and strained quartz crystals.

Table 2: Mechanical results of the investigated samples.

Bulk sample No.	Sample No.	UCS (MPa)	UTS (MPa)	Cohesion (C) (MPa)	Angle of Internal Friction (Φ)	τ	Point load Index $I_{s(50)}$
Bulk sample A	A-1	36	7.4	8.16	41°	24	These samples are not analyzed for point load Index.
	A-2	37	8.3	8.76	39°	28	
	A-3	38.5	8.8	9.82	42°	29	
	A-4	36.5	7.8	8.43	40°	24	
	A-5	36.5	7.4	8.21	42°	22	
Bulk sample B	B-1	39	8.8	9.26	39°	25	
	B-2	40.5	7.8	8.88	43°	25	
	B-3	39	9.8	9.77	37°	26	
Bulk sample C	C-1	42	10.3	10.39	37°	24	
	C-2	43	10.8	10.77	37°	24	
Bulk sample D	D-1	42.2	8	9.14	43°	21	5.66
	D-2	39.6	5.7	7.5	49°	22	4.15
Bulk sample E	E-1	31.5	4.8	6.15	47°	23.5	1.98
	E-2	38.9	4.8	7.01	53°	24	2.53
	E-3	28.8	5.3	6.22	43°	20	2.24

A gel forms that absorbs water, increases in volume, and generates expansive pressure, ultimately leading to concrete failure. Even minimal silica content within the aggregate matrix can act as a source of reactive ASR (Beyene et al., 2013). The studied specimens' analyses are shown in Figure 8 and Table 3.

4.2.7. Alkali-Carbonate Reaction in Aggregate Concrete (ASTM C 586)

ACR is widely employed in geology and civil engineering to assess whether specific rocks or aggregates can react with alkalis and subsequently damage concrete structures. Concrete may expand and crack as a result of this reaction, affecting the structural stability of buildings and other concrete structures (Thomas et al., 2013). ACR happens when the aggregate carbonate components, including dolomite ($CaMg(CO_3)_2$), react with the alkalis in the concrete pore solution. This reaction produces brucite ($Mg(OH)_2$), calcite ($CaCO_3$), and soluble salts. The results are given in Figure 9 and Table 3.

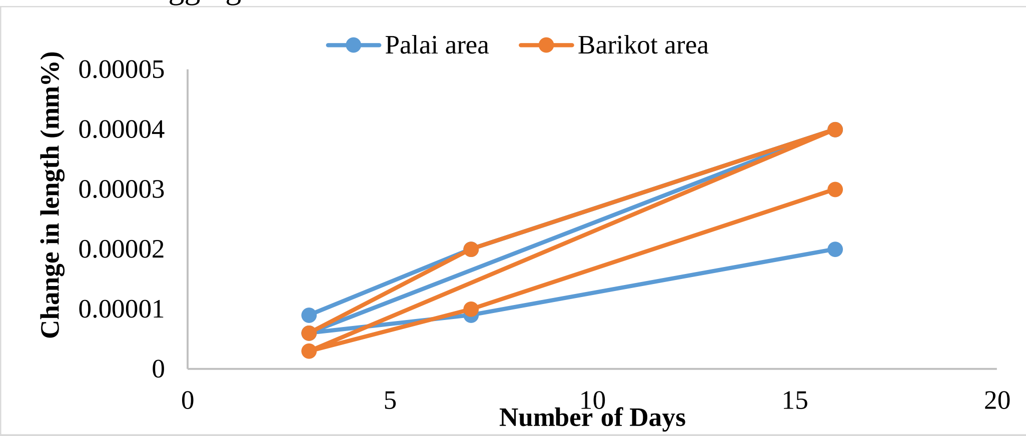

Fig. 8. Change in length due to ASR reactivity.

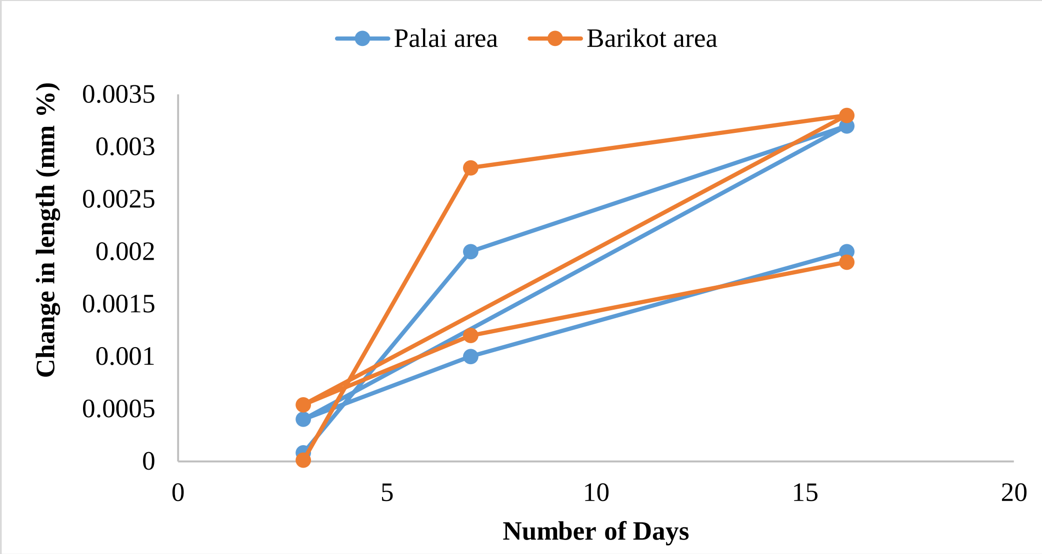

Fig. 9. Change in length due to ACR reactivity.

Table 3: Chemical analysis of selected samples.

Tests	**ASR**				**ACR**			**Soundness**
Sample No.	Length of sample	After 3 days % differences	After 7 days % differences	After 16 days % differences	After 3 days % differences	After 7 days % differences	After 16 days % differences	Actual Loss %
P1	306	0.00001	0.00002	0.00004	0.00008	0.00200	0.00320	3.8
P2	306	0.00001	0.00001	0.00002	0.00040	0.00100	0.00200	
S1	306	0.00001	0.00600	0.00004	0.00001	0.00280	0.00330	1.1
S2	306	0.00000	0.00400	0.00003	0.00054	0.00120	0.00190	

4.2.8. Los Angeles Abrasion Tests (ASTM C 131)

The LAA test measures the weight loss of aggregates resulting from the impact of metallic balls. In this investigation, the LAA test was conducted to determine the maximum wear, thereby providing an assessment of aggregate hardness and strength. A coarse-grained rock has a higher percentage weight loss than a fine-grained rock. (Shakoor and Bonelli, 1991). The obtained results from studied samples are given in Table 4.

4.2.9. Porosity (ASTM C 830)

Porosity refers to the percentage of total void spaces in a rock. The porosity of a rock is determined by factors like grain size, grain shape, and mineralogical composition, particularly the presence of clay minerals (Bell, 1978). The strength of a rock decreases as its porosity increases. In the current research, the porosity of samples was determined by the saturation method (Harrison, 1993). The detailed results are given in Table 4.

4.2.10. Specific gravity (ASTM C 127-88)

Determining the specific gravity of a rock is essential because it has a significant impact on the rock strength and quality. Stronger rocks have a higher specific gravity than weaker ones. Specific gravity is defined as the weight of a particular volume of rock sample divided by the weight of an equal volume of water, or the weight of a certain volume of material divided by an equal quantity of purified water. The unit weight of rock is determined by its porosity, water content, and specific gravity (Anjum et al., 2018). For heavy construction, rocks having a specific gravity higher than 2.25 are considered suitable (Naeem et al., 2019). The sample results are given in Table 4.

4.2.11. Water absorption (ASTM C 127-88)

It relates to how much water a rock sample may easily absorb. Water absorption gives an idea about the strength of rocks. In general, rock samples with high water absorption values are deemed inappropriate for construction. The majority of rocks get weaker through water absorption. The water absorption capacity of a sample is determined by the amount of water it absorbs during 24 hours. The degree and pace of weathering are increased when tiny areas of rock near an exposed surface are mechanically disrupted by repeated hydration and dehydration (Sajid and Arif, 2015). Low water absorption values often indicate a rock's great resilience to weathering; this kind of rock is expected to exhibit very little disintegration impact from chemical weathering and frost action (Naeem et al., 2019). Water absorption is an important feature in determining the longevity of rocks used as construction materials (Sajid and Arif, 2015). Table 4 shows the detailed results from selected samples.

4.2.12. Aggregate Impact Value Test (BS 882)

The primary mechanical qualities required for road stone under current conditions are strong resistance to surface abrasion during traffic and enough resistance to crushing beneath the roller during construction (Bell, 1978). The aggregate impact value measures how resilient the particles are against impacts. The aggregate's ability to withstand breaking under repeated contact is known as the aggregate impact value. Road surfaces are often uneven, and aggregate materials are prone to fragmentation under vehicular loads. Aggregates for construction should thus be durable enough to withstand friction from such collisions. Therefore, impact value is a prime method of assessing the strength of the aggregates to be used in road construction. The detailed results are given in Table 4.

Table 4: Physical analysis of selected samples.

Bulk sample No.	Sample No.	Porosity	Specific gravity	Water absorption	Loss Angles Abrasion	Impact value
Bulk sample ‘‘A’’	A-1	1.82	2.66	0.70	30%	18.3%
	A-2	1.87	2.85	0.66		
	A-3	1.75	2.66	0.67		
	A-4	1.73	2.83	0.90		
	A-5	1.77	2.69	0.67		
Bulk sample ‘B’’	B-1	1.95	2.73	0.73	Not performed for Bulk samples B and C	Not performed for Bulk samples B and C
	B-2	1.77	2.88	0.63		
	B-3	2.02	2.67	0.77		
Bulk sample ‘‘C’’	C-1	1.85	2.69	0.70		
	C-2	1.82	2.85	0.65		
Bulk sample ‘‘D’’	D-1	1.31	2.54	0.12	24%	17%
	D-2	1.51	2.57	0.37		
Bulk sample ‘‘E’’	E-1	1.49	2.31	0.688	Not performed for Bulk sample E	Not performed for Bulk sample E
	E-2	1.67	2.62	0.49		
	E-3	2.49	2.61	0.24		

5. Discussions

Calcite is the dominant constituent in the studied samples (Table 1), and most of the calcite is recrystallized (Figs. 3a, 4b), which represents the deformation event or pro-grade metamorphism in the study area. Plagioclase is the second dominant constituent (Table 1) with remarkable polysynthetic twinning (Figs. 3b, 4d). The accessory minerals are epidote, muscovite, biotite, and quartz. According to the International Society for Rock Mechanics (ISRM) and the Geological Society (Anon, 1977; Table 5), the UCS values in the current research (28.8-42 MPa) classify them as moderate and moderately strong (see Table 5 for comparison).

The Mohr circles with fundamental parameters like cohesion (C) and angle of internal friction (φ) determine shear strength and failure behavior of materials and are best reflected in Figures 5-7. These parameters are crucial for designing stable structures and predicting the behavior of materials under stress, as reflected in the shape and position of the Mohr circle. One effective way to ascertain the strength characteristics of intact rock from drill core samples is to use the point load test. This test is now recognized in geotechnical assessments. According to Bieniawski (1984), point load index (1.98-5.66) is considered low to high strength.

According to the ASTM C 88 soundness standard value for sodium sulphate (Na_2SO_4) are 6-16% and for magnesium sulphate (Mg_2SO_4) are 9-20%, while the analyzed aggregate results are 3.8% and 1.1%, which are suitable for road construction (Table 3). Certain reactive mineral components, such as strained SiO_2 and $CaMg(CO_3)_2$, react with alkalis to produce the ASR and ACR, respectively (Zorlu et al., 2008; Sanchez et al., 2014).

These studies found that the minerals in cement concrete are considered innocuous, with ASR 0.000033% and ACR 0.0026%, which have threshold values of 0.10% (Figs. 8 and 9; Table 3). The low ASR values indicate that the samples contain minimal reactive siliceous components, suggesting that such components are not prevalent in ACR reactive aggregates (cf. Beyene et al., 2013).

Furthermore, the predominance of metamorphism and the presence of recrystallized calcite in most of the Kashala Formation may contribute to the observed low ACR values. This aggregate can be utilized in concrete applications, including dams, pavements, and other large-scale construction projects. The aggregate materials are mostly utilized as a wearing course for roads, or they are employed in concrete based on percentage loss. The analyzed samples have a total loss of 30% and 24% (Table 4), which are suitable for the wearing course of roads (ASTM C 131).

The presence of void spaces significantly influences the behavior and properties of materials, as even minor changes in void space can substantially decrease strength. Accordingly, water absorption of 0.60% and porosity of 1.79% were measured to accurately assess the rock sample's strength.

According to the BS 882 standard, aggregates with an impact value of more than 35% would be considered too weak to be used on road surfaces. The analyzed aggregate impact value is 17.6%, which is within the allowable range for road construction. There are differences in the values of correlations between UCS and calcite (%), UCS and water absorption, UCS and specific gravity, specific gravity and water absorption, UCS and UTS, and UCS and porosity.

The rocks with irregular arrangement of grains in their composition show a higher tendency in terms of their strength than rocks with regular pattern of grain arrangement. This is the reason why the irregular arrangement of minerals in rocks shows strong contact between grains in rocks (Arif et al., 2013).

The strength of rocks decreases with increasing grain size, i.e., the fine-grained rock will show high strength as compared to coarse-grained rocks. (Sajid and Arif, 2015). These recrystallized calcite samples showed a positive relation between UCS and calcite due to irregular contact of grains (Fig. 10a). The samples showed a negative correlation between the UCS and water absorption (Fig. 10b).

It is clear from the analysis that an increase in water absorption reduces the strength of rock in terms of UCS values (Sajid and Arif, 2015). Similarly, the strength of rock is also affected by the recrystallization of minerals.

In addition, variation in shapes and sizes of essential minerals, preferred arrangement of flaky minerals, and percentage of pore spaces can also ultimately affect the rock strength (Sajid and Arif, 2015). From the current research, investigated samples show a positive relation between UCS and specific gravity (Fig. 10c). Furthermore, the presence of water in a rock sample also affects the specific gravity of the material. There is a negative relationship between specific gravity and water absorption (Fig. 10d). Similarly, all the investigated samples showed a positive relation between UTS and UCS (Fig. 10e). The UCS and porosity showed negative relation (Fig. 10f). The value R^2 also called as coefficient of determination defines how to close the data are regression line or the coefficient of multiple determination for multiple regression.

6. Conclusions

The petrographic and geotechnical analysis of metamorphosed calcitic marble from the Kashala Formation reveals several key findings.

- Petrographic studies indicate that calcite is the most dominant constituent, accompanied by plagioclase, muscovite, and biotite, while opaque minerals and quartz are present in trace amounts. The irregular arrangement of grains showed strong contact.
- The recrystallization of calcite and the alteration of plagioclase provide evidence of deformation or prograde metamorphism in the region.
- The petrographic and geotechnical analysis of Kashala Formation showed no deleterious material that can cause alkali-aggregate reactions.
- All the physico-mechanical test results of the research area are within the different international standards range and hence can be strongly recommended for the construction of any structure.
- Overall, the studied rocks are suitable as a source for road, concrete, and other engineering applications.

Table 5: Standard for rock grading based on unconfined compressive strength (Bell, 2007).

Geological Society		**IAEG***		**ISRM****	
(Anon, 1977)		**(Anon, 1979)**		**(Anon, 1981)**	
Description	UCS (MPa)	Description	UCS (MPa)	Description	UCS (MPa)
Very weak	<1.25	Weak	<15	Very low	<6
Weak	1.25-5.0	Moderately weak	15-50	Low	06-Oct
Moderately weak	5.0-15.50	Strong	50-120	Moderate	20-60
Moderately strong	15.50-50	Moderately Strong	120-230	High	60-200
Strong	50-100	Extremely Strong	Over 230	Very High	Over 200
Very strong	100-200				
Extremely strong	Over 200				

IAEG International Association for Engineering Geology*
*ISRM** International Society for Rock Mechanics*

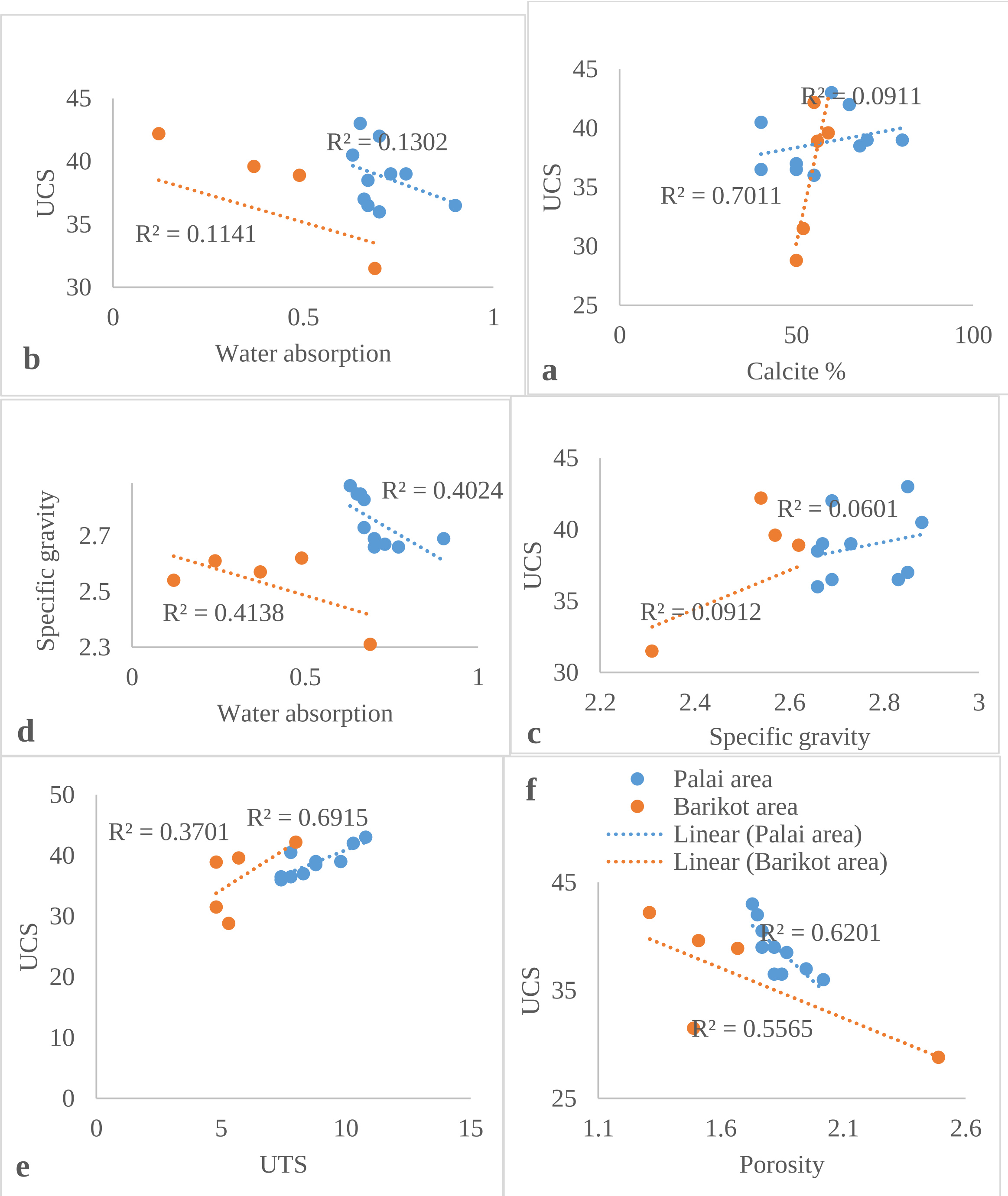

Fig. 10. Correlation between (a) Calcite vs UCS (b) Water absorption vs UCS (c) Specific gravity vs UCS (d) Water absorption vs Specific gravity (e) UTS vs UCS (f) Porosity vs UCS.

Acknowledgement

The authors express their gratitude to the Department of Geology, Bacha Khan University Charsadda, for providing the necessary fieldwork and thin section preparation facilities. The authors also thank the National Centre of Excellence in Geology and Pakistan Council of Scientific and Industrial Research for providing facilities in Geotechnical laboratories.

Authors Contribution

Sami Ullah prepared the project in consultation with Rafique Ahmad. Sami Ullah and Rafique Ahmad jointly wrote the manuscript. Asher Samuel Bhatti *contributed to the revision and editing of the main manuscript. Fahad Ali assisted in the interpretation of the results. Badshah Hussain participated in fieldwork, including sample collection and sample preparation for laboratory analyses. Manzoor Ahmad helped in corel draw work for diagrams and figures.*

References

Afridi, M. I. (2004). Mineral development profile of North West Frontier Province and the role of Directorate General Mines and Minerals in mineral resources development. *Journal of Himalayan Earth Sciences*, *37*(1), 139–154.

Ahmad, Z. (1969). *Directory of mineral deposits of Pakistan* (Geological Survey of Pakistan Record No. 15, pp. 1–200). Geological Survey of Pakistan.

Anjum, M. N., Ali, N., Rehman, Z., Ghayas, M., & Ahmad, W. (2018). Rock aggregate potential of limestone units in the Khyber Formation, Pakistan. *International Journal of Economic and Environmental Geology*, *9*(4), 26–33. https://doi.org/10.46660/ijeeg.v9i4.665

Geological Society Engineering Group Working Party. (1977). The description of rock masses for engineering purposes. *Quarterly Journal of Engineering Geology and Hydrogeology*, *10*, 355–388. https://doi.org/10.1144/GSL.QJEG.1977.010.04.01

IAEG Commission on Engineering Geological Mapping. (1979). Classification of rocks and soils for engineering geological mapping. Part I: Rock and soil materials. *Bulletin of the International Association of Engineering Geology*, *19*, 364–371.

International Society for Rock Mechanics Commission on Classification of Rocks and Rock Masses. (1981). Basic geotechnical description of rock masses. *International Journal of Rock Mechanics and Mining Sciences & Geomechanics Abstracts*, *18*, 85–110. https://doi.org/10.1016/0148-9062(81)90277-1

Arif, M., Bukhari, S. W. H., Muhammad, N., & Sajid, M. (2013). Petrography and physicomechanical properties of rocks from the Ambela granitic complex, NW Pakistan. *The Scientific World Journal*, *2013*, Article 349381. https://doi.org/10.1155/2013/349381

ASTM International. (2001). *Standard test method for potential alkali reactivity of aggregates (mortar-bar method)* (ASTM C1260-01). https://doi.org/10.1520/C1260-01

ASTM International. (2001). *Standard test method for specific gravity and absorption of coarse aggregate* (ASTM C127-88).

ASTM International. (2001). *Standard test method for resistance to degradation of small-size coarse aggregate by abrasion and impact in the Los Angeles machine* (ASTM C131-01). https://doi.org/10.1520/C0131-01

ASTM International. (1999). *Standard test method for potential alkali reactivity of carbonate rocks for concrete aggregates (rock cylinder method)* (ASTM C586-99). https://doi.org/10.1520/C0586-99

ASTM International. (2006). *Standard test methods for apparent porosity, liquid absorption, apparent specific gravity, and bulk density of refractory shapes by vacuum pressure* (ASTM C830-00(2006)). https://doi.org/10.1520/C0830-00R06

ASTM International. (1999). *Standard test method for soundness of aggregates by use of sodium sulfate or magnesium sulfate* (ASTM C88-99).

ASTM International. (2016). *Standard test method for splitting tensile strength of intact rock core specimens* (ASTM D3967-16). https://doi.org/10.1520/D3967-16

ASTM International. (2008). *Standard test method for determination of the point load strength index of rock and application to rock strength classifications* (ASTM D5731-08). https://doi.org/10.1520/D5731-08

ASTM International. (2014). *Standard test methods for compressive strength and elastic moduli of intact rock core specimens under varying states of stress and temperatures* (ASTM D7012-14). https://doi.org/10.1520/D7012-14

Basu, A., & Aydin, A. (2006). Predicting uniaxial compressive strength by point load test: Significance of cone penetration. *Rock Mechanics and Rock Engineering*, *39*, 483–490. https://doi.org/10.1007/s00603-006-0082-y

Bell, F. G. (1978). The physical and mechanical properties of the Fell sandstones, Northumberland, England. *Engineering Geology*, *12*, 1–29. https://doi.org/10.1016/0013-7952(78)90002-9

Bell, F. G. (2007). *Engineering geology*. Elsevier.

Beyene, M., Snyder, A., Lee, R. J., & Blaszkiewicz, M. (2013). Alkali silica reaction (ASR) as a root cause of distress in a concrete made from alkali carbonate reaction (ACR) potentially susceptible aggregates. *Cement and Concrete Research*, *51*, 85–95. https://doi.org/10.1016/j.cemconres.2013.04.014

Bieniawski, Z. (1984). The design process in rock engineering. *Rock Mechanics and Rock Engineering*, *17*(3), 183–190.

Bieniawski, Z. T. (1989). *Engineering rock mass classifications: A complete manual for engineers and geologists in mining, civil, and petroleum engineering*. John Wiley & Sons.

Brook, N. (1985). The equivalent core diameter method of size and shape correction in point load testing. *International Journal of Rock Mechanics and Mining Sciences & Geomechanics Abstracts*, *22*(2), 61–70. https://doi.org/10.1016/0148-9062(85)92328-9

British Standards Institution. (1992). *Specifications for aggregates from natural sources for concrete and roadstones* (BS 882:1992). British Standards Institution.

Chau, K. T., & Wong, R. H. C. (1996). Uniaxial compressive strength and point load strength of rocks. *International Journal of Rock Mechanics and Mining Sciences & Geomechanics Abstracts*, *33*(2), 183–188. https://doi.org/10.1016/0148-9062(95)00056-9

ASTM International. (2000). *Standard test methods for apparent porosity, liquid absorption, apparent specific gravity, and bulk density of refractory shapes by vacuum pressure* (ASTM C830-00). https://doi.org/10.1520/C0830-00

Coward, M. P., Rex, D. C., Asif Khan, M., Windley, B. F., Broughton, R. D., Luff, I. W., Petterson, M. G., & Pudsey, C. J. (1986). Collision tectonics in the NW Himalayas. *Geological Society, London, Special Publications*, *19*(1), 203–219. https://doi.org/10.1144/GSL.SP.1986.019.01.13

Dhuime, B., Bosch, D., Bodinier, J.-L., Garrido, C. J., Bruguier, O., Hussain, S. S., & Dawood, H. (2007). Multistage evolution of the Jijal ultramafic–mafic complex (Kohistan, N Pakistan): Implications for building the roots of island arcs. *Earth and Planetary Science Letters*, *261*(1–2), 179–200. https://doi.org/10.1016/j.epsl.2007.06.026

Din, F., Rafiq, M., & Mohammad, N. (1993). Strength properties of various building stones of NWFP, Pakistan. *Journal of Himalayan Earth Sciences*, *26*(1), 119–126.

DiPietro, J. A. (1990). *Stratigraphy, structure, and metamorphism near Saidu Sharif, Lower Swat, Pakistan* [Doctoral dissertation, Oregon State University].

Ghosh, D. K., & Srivastava, M. (1991). Point-load strength: An index for classification of rock material. *Bulletin of the International Association of Engineering Geology*, *44*(1), 27–33. https://doi.org/10.1007/BF02602707

DiPietro, J. A., Hussain, A., Ahmad, I., & Khan, M. A. (2000). The Main Mantle Thrust in Pakistan: Its character and extent. *Geological Society, London, Special Publications*, *170*(1), 375–393. https://doi.org/10.1144/GSL.SP.2000.170.01.20

DiPietro, J. A., Pogue, K. R., Lawrence, R. D., Baig, M. S., Hussain, A., & Ahmad, I. (1993). Stratigraphy south of the Main Mantle Thrust, Lower Swat, Pakistan. *Geological Society, London, Special Publications*, *74*(1), 207–220. https://doi.org/10.1144/GSL.SP.1993.074.01.15

Harrison, D. J. (1993). *Industrial minerals laboratory manual: Limestone* (Technical Report WG/92/29, Mineralogy and Petrology Series). British Geological Survey.
Hartley, A. (1974). A review of the geological factors influencing the mechanical properties of road surface aggregates. *Quarterly Journal of Engineering Geology, 7*(1), 69–100. https://doi.org/10.1144/GSL.QJEG.1974.007.01.05
Hussain, M. F., Mondal, M. E. A., & Ahmad, T. (2004). Geodynamic evolution and crustal growth of the Central Indian Shield: Evidence from geochemistry of gneisses and granitoids. *Journal of Earth System Science, 113*(4), 699–714. https://doi.org/10.1007/BF02704030
Jaeger, J. C., & Cook, N. G. W. (1976). *Fundamentals of rock mechanics* (2nd ed.). Chapman and Hall.
Jan, M. Q., & Howie, R. A. (1981). The mineralogy and geochemistry of the metamorphosed basic and ultrabasic rocks of the Jijal Complex, Kohistan, NW Pakistan. *Journal of Petrology, 22*(1), 85–126. https://doi.org/10.1093/petrology/22.1.85
Johnson, R. B., & DeGraff, J. V. (1988). *Principles of engineering geology*. John Wiley & Sons.
Jumikis, A. R. (1983). *Rock mechanics* (2nd ed.). Trans Tech Publications.
Kazmi, A. H., & Abbas, S. G. (2001). *Metallogeny and mineral deposits of Pakistan*. Orient Petroleum Incorporated.
Kazmi, A., Lawrence, R., Dawood, H., Snee, L., & Hussain, S. (1984). Geology of the Indus suture zone in the Mingora–Shangla area of Swat. *Geological Bulletin of the University of Peshawar, 17*.
Khan, M. A., Stern, R. J., Gribble, R. F., & Windley, B. F. (1997). Geochemical and isotopic constraints on subduction polarity, magma sources, and palaeogeography of the Kohistan intra-oceanic arc, northern Pakistan Himalaya. *Journal of the Geological Society, 154*(6), 935–946. https://doi.org/10.1144/gsjgs.154.6.0935
Khan, M. W., Sultan, S. A., Iftikhar, A., & Izhar, M. S. (2017). Petrographic and geochemical analyses of Kirana Hills Shield rocks around Sargodha and economic potential. *International Journal of Economic and Environmental Geology, 8*(2), 9–20.
Koukis, G., Sabatakakis, N., & Spyropoulos, A. (2007). Resistance variation of low-quality aggregates. *Bulletin of Engineering Geology and the Environment, 66*, 457–466. https://doi.org/10.1007/s10064-007-0098-x
Lees, G., & Kennedy, C. K. (1975). Quality, shape and degradation of aggregates. *Quarterly Journal of Engineering Geology, 8*(3), 193–209. https://doi.org/10.1144/GSL.QJEG.1975.008.03.03
Naeem, M., Zafar, T., Touseef Bilal, M., & Oyebamiji, A. (2019). Physical characterization and alkali carbonate reactivity (ACR) potential of the rocks from Bauhti Pind and Bajar area, Hassan Abdal, Pakistan. *SN Applied Sciences, 1*(7), 696. https://doi.org/10.1007/s42452-019-0736-5
Ringuette, L., Martignole, J., & Windley, B. F. (1999). Magmatic crystallization, isobaric cooling, and decompression of the garnet-bearing assemblages of the Jijal sequence (Kohistan terrane, western Himalayas). *Geology, 27*(2), 139–142. https://doi.org/10.1130/0091-7613(1999)027<0139>2.3.CO;2
Sajid, M., & Arif, M. (2015). Reliance of physico-mechanical properties on petrographic characteristics: Consequences from the study of Utla granites, north-west Pakistan. *Bulletin of Engineering Geology and the Environment, 74*, 1321–1330. https://doi.org/10.1007/s10064-014-0690-9
Sanchez, L. F., Multon, S., Sellier, A., Cyr, M., Fournier, B., & Jolin, M. (2014). Comparative study of a chemo–mechanical modeling for alkali silica reaction (ASR) with experimental evidences. *Construction and Building Materials, 72*, 301–315. https://doi.org/10.1016/j.conbuildmat.2014.09.007

Schaltegger, U., Zeilinger, G., Frank, M., & Burg, J.-P. (2002). Multiple mantle sources during island arc magmatism: U–Pb and Hf isotopic evidence from the Kohistan arc complex, Pakistan. *Terra Nova*, *14*(6), 461–468. https://doi.org/10.1046/j.1365-3121.2002.00432.x

Searle, M. P., Khan, M. A., Fraser, J. E., Gough, S. J., & Jan, M. Q. (1999). The tectonic evolution of the Kohistan–Karakoram collision belt along the Karakoram Highway transect, north Pakistan. *Tectonics*, *18*(6), 929–949. https://doi.org/10.1029/1999TC900042

Shakoor, A., & Bonelli, R. E. (1991). Relationship between petrographic characteristics, engineering index properties, and mechanical properties of selected sandstones. *Environmental & Engineering Geoscience*, *28*(1), 55–71. https://doi.org/10.2113/gseegeosci.xxviii.1.55

Small and Medium Enterprise Development Authority. (2007). *Pre-feasibility study: Marble and onyx products manufacturing* (Document No. 21). Government of Pakistan.

Smith, M. R., & Collis, L. (Eds.). (2001). *Aggregates: Sand, gravel and crushed rock aggregates for construction purposes* (3rd ed., Geological Society Engineering Geology Special Publication No. 17). Geological Society.

Thomas, M. D. A., Fournier, N., & Folliard, K. J. (2013). *Alkali-aggregate reactivity (AAR) facts book*. Federal Highway Administration.

Tuğrul, A., & Zarif, I. H. (1999). Correlation of mineralogical and textural characteristics with engineering properties of selected granitic rocks from Turkey. *Engineering Geology*, *51*(4), 303–317. https://doi.org/10.1016/S0013-7952(98)00071-4

Whitney, D. L., & Evans, B. W. (2010). Abbreviations for names of rock-forming minerals. *American Mineralogist*, *95*(1), 185–187. https://doi.org/10.2138/am.2010.3371

Wu, Y., Parker, F., & Kandhal, P. S. (1998). Aggregate toughness/abrasion resistance and durability/soundness tests related to asphalt concrete performance in pavements. *Transportation Research Record*, *1638*(1), 85–93. https://doi.org/10.3141/1638-10

Xeidakis, G. S., & Samaras, I. S. A. (1996). A contribution to the study of some Greek marbles. *Bulletin of the International Association of Engineering Geology*, *53*(1), 121–129.

Zorlu, K., Gökçeoglu, C., Ocakoglu, F., Nefeslioglu, H. A., & Acikalin, S. (2008). Prediction of uniaxial compressive strength of sandstones using petrography-based models. *Engineering Geology*, *96*(3–4), 141–158. https://doi.org/10.1016/j.enggeo.2007.10.009